The actin-binding protein α-adducin is required for maintaining axon diameter

Sérgio Carvalho Leite[1,3,4], **Paula Sampaio**[2,3], **Vera Filipe Sousa**[1,3,4], **Joana Nogueira-Rodrigues**[1,3], **Rita Pinto-Costa**[1,3], **Luanne Laurel Peters**[5], **Pedro Brites**[1,3], and **Mónica Mendes Sousa**[1,3,*]

[1]Nerve Regeneration group, IBMC-Instituto de Biologia Molecular e Celular, Universidade do Porto, 4150-180 Porto, Portugal

[2]Advanced Light Microscopy unit, IBMC-Instituto de Biologia Molecular e Celular, Universidade do Porto, 4150-180 Porto, Portugal

[3]Instituto de Investigação e Inovação em Saúde, Universidade do Porto, 4200-135 Porto, Portugal

[4]ICBAS, Universidade do Porto, 4050-313 Porto, Portugal

[5]The Jackson Laboratory, Bar Harbor, Maine 04609, USA

SUMMARY

The actin-binding protein adducin was recently identified as a component of the neuronal subcortical cytoskeleton. Here we analyzed mice lacking adducin to uncover the function of this protein in actin rings. α-adducin knockout mice presented progressive axon enlargement in the spinal cord, optic and sciatic nerve, followed by axon degeneration and loss. Using stimulated emission depletion super-resolution microscopy, we show that a periodic subcortical actin cytoskeleton is assembled in every neuron type inspected including retinal ganglion cells and dorsal root ganglia neurons. In neurons devoid of adducin, the actin ring diameter increased, although the inter-ring periodicity was maintained. *In vitro*, the actin ring diameter adjusted as axons grew suggesting the lattice is dynamic. Our data support a model in which adducin activity is not essential for actin ring assembly and periodicity, but is necessary to control the diameter of both actin rings and axons, and actin filament growth within rings.

Abstract

Wild Type

α-adducin KO

● ● ● actin   ● adducin   — spectrin tetramer

INTRODUCTION

In neurons, tight regulation of cytoskeleton organization and dynamics has emerged as a key factor in polarization, synaptogenesis, axon growth and degeneration (Kevenaar and Hoogenraad, 2015). Recently, using stochastic optical reconstruction microscopy (STORM), a new view on the neuronal subcortical actin structure organization was proposed (Xu et al., 2013). In cultured hippocampal neurons and in hippocampal slices, actin was shown to form ring-like structures around the axonal circumference with a periodic spacing of 180–190 nm (Lukinavicius et al., 2014; Xu et al., 2013). Neuronal actin rings contain adducin, an actin-capping protein, and are crosslinked by αII/βII spectrin tetramers that contribute to the even spacing between individual rings (Xu et al., 2013). Once assembled, spectrin tetramers in the periodic lattice form a highly stable structure with a slow turnover (Zhong et al., 2014). An axon-specific function has been challenged by the identification of actin rings in dendrites of mature hippocampal neurons (D'Este et al., 2015). Although the function of neuronal actin rings remains largely elusive, they may provide mechanical support for the thin structure of axons and dendrites. Supporting this notion, deletion of β spectrin in *C.elegans* leads to axon breakage upon movement of the worm (Hammarlund et al., 2007).

In addition to βII or βIV spectrins, adducin is the only actin-binding protein found in neuronal actin rings. Mammalian adducins comprise 3 closely related genes (α, β and γ), with α and γ being ubiquitously expressed and β being abundant in brain and erythrocytes (Matsuoka et al., 2000). Functional tetrameric adducin is formed by two heterodimers in which the α monomer is an absolute requirement. Adducin has three main functions as a regulator of the actin cytoskeleton: i) it promotes the bundling of actin filaments, ii) it caps the actin filament barbed ends inhibiting the incorporation of new actin monomers, and iii) it is involved in the recruitment and crosslinking of spectrin to the ends of actin filaments (Li et al., 1998). Adducin is an important molecule in synapse formation, as mouse and fly adducin mutants have decreased synaptic stability (Bednarek and Caroni, 2011; Pielage et

al., 2011). It has been associated with neurodegenerative conditions including amyotrophic lateral sclerosis (Gallardo et al., 2014) and cerebral palsy (Kruer et al., 2013), further supporting an important role in the homeostasis of the actin cytoskeleton in the nervous system.

Here we show that loss of α-adducin *in vivo* causes progressive axon enlargement and degeneration and that, *in vitro*, adducin-deficient neurons have axon actin rings with increased diameters. Our data support a model in which adducin regulates the diameter of actin rings and axons.

RESULTS

α-adducin KO mice develop progressive axon enlargement and degeneration

Functional adducin consists of a tetrameric complex of two heterodimers where the α monomer is essential. Approximately 50% of α-adducin KO mice in the 129S1/SvlmJ;C57BL/6J background develop a lethal hydrocephaly, suggesting a role of adducin, which localizes to the basolateral membranes of choroid plexus epithelial cells, in the maintenance of cerebrospinal fluid homeostasis (Robledo et al., 2008; Robledo et al., 2012). Of note, only the non-hydrocephalous α-adducin KO littermates were used in this study. Nervous tissue from α-adducin KO mice showed severely decreased levels of β- and γ-adducin (Figure S1A), similar to what is observed in erythrocytes from these animals (Robledo et al., 2008). Consistently, in α-adducin KO mouse brains no dimer/tetramer formation was visualized by western blot after native PAGE (Figure S1B). Immunofluorescence of hippocampal neurons further confirmed the nearly complete absence of adducin in α-adducin KO neurons (Figure S1C). In the absence of α-adducin, capping protein (EcapZ) levels were similar to those found in WT animals (Figure S1D) and no significant statistical differences were seen for βII spectrin levels (Figure S1E and S1F). Moreover, the axonal/dendritic distribution of spectrin in α-adducin KO hippocampal neurons was similar to that found in WT neurons (Figure S1G and S1H). The absence of adducin did not impair axon specification and neuron polarity (Figure S1I and S1J) and it did not significantly affect axon or dendrite length (Figure S1K-M).

To further understand the function of adducin in neuron biology, we analyzed the central and peripheral nervous system of α-adducin KO mice. In the central nervous system, deletion of α-adducin led to axon loss in both the optic nerve (Figure 1A and 1B) and the spinal cord (Figure 1G and 1H). In the optic nerve, axon loss was progressive since normal axon density was observed at postnatal day 20 (P20), but by P100 α-adducin KO optic nerves had a 40% reduction in axon density (Figure 1B). At this age, we also observed severe nerve atrophy (Figure 1C) with a 33% decreased optic nerve area in mutant nerves. Overall, the decrease in axon density and reduced nerve cross-sectional area resulted in an estimated loss of 50% of the total number of axons in α-adducin KO optic nerves (P100, WT: $65,546 \pm 6,771$ axons/nerve, n=5; and α-adducin KO: $33,805 \pm 13,528$ axons/nerve, n=4; p<0.01). Decreased axon density was also found in α-adducin KO spinal cords. Analysis of the corticospinal tract (CST) revealed a 25% loss of axon density in the absence of α-adducin (Figure 1G and 1H). In the peripheral nervous system, we also observed a decreased density of myelinated axons in sciatic nerves from α-adducin KO mice (P20, WT: $46,993 \pm 5,325$ axons/mm^2, n=3; and

α-adducin KO: 38,600 ± 3,523 axons/mm^2, n=3; p<0.05). Combined, these results reinforce earlier findings in the PNS of these mutants (Robledo et al., 2012), and highlight that loss of adducin has a major impact in central and peripheral nervous system axons.

Progressive axon enlargement preceded axon loss in α-adducin KO mice. Distribution of axons of different diameters was normal in the P20 optic nerve, but we observed an increase in high diameter axons (>2 μm) at P60. This effect was even more pronounced at P100, with an overall decrease in small diameter axons accompanied by an increase in large diameter axons (Figure 1D–1F). Interestingly, myelin thickness, calculated as the g-ratio, was similar in the optic nerve of P100 WT and α-adducin KO mice (WT: 0.76 ± 0.03, n=5; α-adducin KO: 0.77 ± 0.02, n=4, p=0.58) suggesting that enlarged axons were normally myelinated. Similar to the optic nerve, the spinal cord of α-adducin KO mice displayed decreased numbers of small diameter axons and an increase in large diameter axons (Figure 1G, asterisks and Figure 1I). In the sciatic nerve, abnormally enlarged axons with a diameter over 10 μm were found only in α-adducin KO mice (Figure 1J, asterisks), although there was no change in the overall distribution of axon diameter for axons with a diameter under 8 μm. Together, this data suggest that the increase in axon size is not due to a preferential loss of small axons, but instead that all classes of axons can be affected leading to the appearance of abnormally enlarged axons with diameters that are not found in WT nerves. In summary, in the absence of adducin, there is an increase in axon diameter and axonal loss both in the CNS and PNS.

Loss of adducin impairs cytoskeleton dynamics in the growth cone and axonal transport

Cytoskeleton deregulation is generally related to axon enlargement and axonopathy. Therefore, we examined the effects of α-adducin depletion on the axonal cytoskeleton. Optic nerve axons from P100 α-adducin KO had a constant diameter as observed in longitudinal sections, without focal enlargements or noticeable accumulation of organelles (Figure 2A), and with normal density of microtubules and neurofilaments (Figure 2B and 2C). *In vitro*, the growth cones of α-adducin KO hippocampal (Figure 2D and 2E) and DRG neurons (Figure S2A and S2B) had increased actin retrograde flow as determined by transfection with LifeAct-GFP (Riedl et al., 2008). These results suggest that loss of the actin-capping activity of adducin has a direct impact on the growth of actin filaments, which may affect the coordinated interplay with microtubule dynamics at the growth cone (Coles and Bradke, 2015; Flynn et al., 2012). In fact, we observed that following transfection with the microtubule *plus*-end tracking protein, end-binding protein 3 (EB3)-GFP (Stepanova et al., 2003), the growth speed of microtubules was increased in α-adducin KO growth cones (Figure 2F and 2G), which showed comets with the same duration but with increased length (Figure 2H and 2I). Combined, these results suggest a synergistic effect of increased actin dynamics and microtubule invasion and growth. Although more dynamic, growth cones of α-adducin KO neurons were morphologically similar to those of WT neurons and displayed comparable amounts of F-actin (Figure S2C and S2D).

As changes in cytoskeleton dynamics and axon enlargement are largely related to impaired axonal transport, we compared the movement of organelles and synaptic vesicles in WT and α-adducin KO hippocampal and DRG neurons. In hippocampal neurons, the absence of

adducin affected the speed of axonal transport of mitochondria (Figure 2J and 2K) and lysosomes (Figure 2L and 2M). Despite the decreased speed of axonal transport in both the anterograde and retrograde directions, we did not observe a consistent effect in the percentage of moving cargos (Figure S2K–2M). Interestingly, no difference in the speed of transport of synaptic vesicles was observed (Figure 2N and 2O). In DRG neurons, similar findings were observed, both for organelle transport speed (Figure S2E–S2J) and in the percentage of moving cargos (Figure S2N–S2P).

Adducin is essential for the maintenance of axonal diameter

Recently, adducin was shown to be a component of actin rings in hippocampal neurons (Xu et al., 2013). The development of silicon rhodamine actin (SiR-actin), in combination with stimulated emission depletion (STED) microscopy, allowed for the detection of actin rings in axons, dendrites and at the nodes of Ranvier (D'Este et al., 2015). The function of this novel structure of the neuronal actin cytoskeleton remains elusive, and it is not known if these structures are found in other neurons. Using SiR-actin and STED microscopy, we show that DRG neurons (Figure 3A) and retinal ganglion cell neurons (RGC) (Figure 3D) also assemble actin rings, with a conserved spacing of approximately 190 nm. In DRG neurons, the ring periodicity was 194.4 ± 0.5 nm (Figure 3B). Throughout the axon shaft of DRG neurons, parallel long actin fibers were visible in axons (Figure 3C), in line with what was reported in hippocampal neurons (D'Este et al., 2015; Ganguly et al., 2015).

The role of adducin in actin ring formation and organization is still unknown. Given the different functions of adducin in the regulation of the actin-spectrin cytoskeleton, we hypothesized that in its absence the periodic pattern of rings would be disrupted. This could result from decreased crosslinking of actin-spectrin junctions, and/or aberrant F-actin filament size due to lack of adducin's capping activity, leading to an enlarged ring diameter. In retina explant cultures, WT RGC presented a 188.7 ± 4.5 nm actin ring periodicity (Figure 3D, 3F and 3H). α-adducin KO axons also assembled actin rings with a similar periodicity (187.3 ± 5.0 nm) (Figure 3E, 3G and 3H). These data suggest that the N-terminus actin-binding domain of spectrin is probably sufficient for actin ring binding to the spectrin lattice.

In the model proposed for actin ring organization (Xu et al., 2013), each ring is composed of several short and stable actin filaments capped at their barbed ends by adducin. Removal of the capping protein is predicted to dysregulate actin filament length, resulting in increased filament size and consequently in an increased diameter of the neuronal actin rings. Supporting this hypothesis, in α-adducin KO RGC axons, actin rings had a 1.3 fold increase in diameter (Figure 3I). Interestingly, the increase in actin ring diameter observed in α-adducin KO RGC *in vitro* was similar to the enlargement observed *in vivo* in optic nerve axons (Figure 1A and 1D–1F). Together, our findings support not only the ubiquitous nature of the periodic actin rings in neurons, but also that the capping activity of adducin is required to maintain axonal actin ring diameter.

In hippocampal neurons, the actin ring assembly starts as polarization begins (DIV2/3) from the proximal to the distal axon compartment (Zhong et al., 2014). To evaluate the temporal consequences of depleting adducin, we analyzed WT and α-adducin KO hippocampal

neuron cultures at different time points (DIV 8, 16 and 30). At these time points, dendrites were enriched in actin fibers and actin-enriched dendritic spines laterally, while axons were clearly distinguished by the low abundance of longitudinal actin fibers and absent dendritic spines (Figure 4A). The analysis of the periodic distribution of axonal actin rings from DIV8 to DIV30 revealed that at DIV8 α-adducin KO neurons had an increased periodicity that was normalized from DIV16 onwards (Figure 4B). Although our findings indicate that adducin may have an initial role in the periodic assembly of actin rings, the observation that with time, mutant neurons still acquire normal actin ring periodicity suggests that either adducin has a transient role, or that the spectrin-actin interaction is sufficient to provide the normal distribution of actin rings along axons.

The analysis of DIV8 to DIV30 hippocampal neurons also showed a consistent 1.3-fold increase in actin ring diameter in the absence of adducin (Figure 4C). Interestingly, during the time in culture, both WT and α-adducin KO neurons showed a significant reduction of the actin ring diameter (Figure 4C), which is related to the narrowing of axons over time when in vitro. This finding supports that the actin filaments that compose actin rings are more dynamic than initially suggested, having the capacity to adapt to conditions in which a variation in axonal diameter occurs. Analysis of F-actin content in actin rings throughout time was performed to further analyze the mechanism of progressive constriction. In WT neurons, the mean intensity of actin increased from DIV8 to DIV30 (Figure 4H), suggesting that the decrease in axon diameter is accompanied by the bundling and condensation of actin filaments. In contrast to WT neurons, in α-adducin KO neurons, the mean actin intensity per ring remained unchanged with time in culture. However, α-adducin KO axons at DIV8 had an increased mean actin intensity when compared to DIV8 WT axons. This may result from an increase in uncapped barbed actin ends that could enable an enhanced growth of branched actin filaments. In fact, increased filopodia density occurs upon inhibition of capping activity, as seen in the absence of capping protein (Sinnar et al., 2014). Given that one cannot uncouple the capping/bundling activities of adducin (Mische et al., 1987), it is challenging to determine its precise role in the mechanism of progressive constriction. Since both WT and α-adducin KO neurons are capable of decreasing actin ring diameter over time in culture, the dynamics of the periodic lattice is probably dependent on additional actin-binding proteins, whereas the fine regulation of ring diameter is modulated by the presence of adducin.

DISCUSSION

Up to the discovery of axonal actin waves, actin trails and actin rings, the neuronal actin cytoskeleton had its relevance restricted to growth cones, synaptic structures and the axon initial segment (Roy, 2016). The identification of these novel structures open new exciting prospects on our understanding of neurobiology. Still, the molecular details of ring composition, assembly, maintenance, behavior and function, both under physiological and pathological conditions, are largely unknown. Although molecular detail is still lacking, three core components have been identified in axonal rings: actin, spectrin and adducin (Xu et al., 2013). Here, we show that depletion of adducin *in vivo* leads to a time-dependent axon enlargement and loss, and to increased actin ring diameter *in vitro*. These defects were independent of hydrocephaly, as they occurred irrespectively of ventricle enlargement. As

previously suggested, actin rings are probably made of short adducin-capped actin filaments (Xu et al., 2013; Zhong et al., 2014). Our data supports a model in which the actin-capping and bundling activity of adducin regulates filament growth and thereby ring diameter but is not required for ring assembly and periodicity. In the actin-rich growth cones of α-adducin KO neurons, the actin cytoskeleton is more dynamic, resulting in increased actin retrograde flow during axon extension, presumably as a result of increased incorporation of actin monomers. Similarly, it is possible that the actin filaments found in the axonal actin rings have increased monomer incorporation and filament size. Although the analyses of growth cone actin dynamics and actin rings were performed at different time points, these periodic structures are assembled in the initial stages of polarization, when growth cone dynamics was assessed. In this respect, the crucial role of actin dynamics for the assembly of actin-based periodic structures in different biological contexts was recently discussed (Leite and Sousa, 2016).

The periodic distribution of spectrin and actin is seen at DIV2-3, whereas the presence of adducin in the rings is only visible at DIV8 (Zhong et al., 2014), presumably to stabilize the actin-spectrin lattice as axons mature (Xu et al., 2013; Zhong et al., 2014). The results presented here indicate that the periodic lattice has a more dynamic nature than FRAP analysis of βII spectrin initially suggested (Zhong et al., 2014). In comparison with βII spectrin, actin is probably the most dynamic component of the subcortical neuronal cytoskeleton. *In vitro*, we demonstrate that axons of hippocampal neurons have a progressive decrease in diameter, independent of adducin. This suggests the existence of additional regulatory mechanisms of ring size, probably involving other actin-binding proteins. The analysis throughout time of the F-actin content in the periodic actin rings suggests that adducin may be involved in the regulation of F-actin density in the rings, likely through a combined action of its actin capping and bundling functions.

This duality in dynamism of the different components of the periodic lattice structure would explain why the longitudinal distribution, which is dependent of spectrin spacers of 190 nm, would be stable throughout axon extension/maturation, whereas the ring diameter that depends on the dynamics of the actin filaments that comprise the rings might vary and adapt. Variations in axon diameter also pose interesting questions on the arrangement and stability of the spectrin cytoskeleton. With an enlarged axonal diameter, would spectrins become less dense i.e., more laterally spaced, or would there be an up-regulation of spectrins to keep the density constant? In the absence of adducin, axon enlargement occurs while the total levels of spectrin are maintained. Therefore, and although the direct high resolution measurement of spectrin density is challenging to perform, we would expect, at least in this model, spectrins to be less dense in larger axons and the small actin filaments that compose the rings to have an increased length.

There are several similarities between the spectrin-actin lattice in neurons and erythrocytes. In erythrocytes, spectrin, actin and associated proteins are organized into a stable cortical cytoskeleton, often referred to as the membrane skeleton, that confers strength and elasticity to the red cell (Mohandas and Gallagher, 2008). The absence of adducin results in misshaped erythrocytes that are less resistant to mechanic stresses such as osmotic pressure (Gilligan et al., 1999; Robledo et al., 2008). However, when erythrocytes need to squeeze

through small capillaries, the erythrocyte cortical cytoskeleton becomes dynamic and deformable. In neurons, it would be interesting to assess whether the actin-spectrin lattice is also able to become dynamic in specific contexts such as during axon degeneration and plasticity events as actin rings may be rearranged/disassembled to promote either constriction of the axonal membrane or axon branching.

Could there be a link between axonal actin rings, microtubules and axonal transport? In fact, axonal actin rings are dependent on microtubule integrity as microtubule destabilization with nocodazole leads to loss of actin rings (Zhong et al., 2014). Interestingly, analysis of α-adducin KO neurons revealed a possible link between a more unstable actin cytoskeleton and microtubule dynamics in the growth cone. However, how these different components of the axonal cytoskeleton crosstalk, is unknown. A possible link between actin rings and axonal transport has already been raised (Gallo, 2013). According to this hypothesis, actin rings could serve as docking sites for axonal cargos associated with myosins, which would allow an approximately 200 nm resolution for the control of axonal transport (Gallo, 2013). Supporting this notion, in neurons, mitochondria dock along axons through myosinV, and depletion of myosins results in increased speed and length of microtubule-based runs (Pathak et al., 2010). Would actin rings with an increased diameter, as seen in α-adducin KO neurons, have an increased capacity to 'sequester' myosin motors, decreasing the average speed of axonal transport? The answer to this question, together with several others raised by the identification of these novel ring structures, relies intimately on the identification of the actin-binding proteins that shape actin rings, on their mechanistic assembly, on determining their relevance to the mechanical properties of axons and dendrites, and on the characterization of their organization in the course of axon degeneration.

EXPERIMENTAL PROCEDURES

Animals

α-adducin KO mice and WT littermates were obtained from heterozygous breeding pairs and genotyped as described (Robledo et al., 2008). Mice were handled according to European Union and National legislation.

Cell preparation for STED imaging of axonal actin rings

Actin ring analysis was done using the silicon-rhodamine (SiR)-actin probe (Lukinavicius et al., 2014) and stimulated emission depletion microscopy (Lukinavicius et al., 2014), in a Leica TCS SP8 STED 3X (Leica Microsystems). DIV2 rat DRG neurons, DIV 19 mouse retina explants and DIV8, DIV16 and DIV30 mouse hippocampal neurons were incubated for 1 hour with 2μM SiR-actin (kindly provided by Prof Kai Johnsson, École Polytechnique Fédérale de Lausanne, Switzerland) and fixed 20 minutes in 4% PFA. Samples were initially visualized by confocal and then STED microscopy was performed (see Supplemental Experimental Procedures for details).

Statistical analysis

Animals were randomly assigned for analyses and all measurements were performed with the investigator blinded to the genotype. Data are shown as mean ± s.e.m. Statistical

significance was determined by Student's t test using Prism (GraphPad Software), with exception of actin ring measurements in hippocampal neuron cultures, where one-way ANOVA was used (GraphPad Software).

Supplementary Material

Refer to Web version on PubMed Central for supplementary material.

REFERENCES

Bednarek E, Caroni P. beta-Adducin is required for stable assembly of new synapses and improved memory upon environmental enrichment. Neuron. 2011; 69:1132–1146. [PubMed: 21435558]

Coles CH, Bradke F. Coordinating Neuronal Actin-Microtubule Dynamics. Curr Biol. 2015; 25:R677–691. [PubMed: 26241148]

D'Este E, Kamin D, Göttfert F, El-Hady A, Hell SW. STED Nanoscopy Reveals the Ubiquity of Subcortical Cytoskeleton Periodicity in Living Neurons. Cell Rep. 2015:10.

Flynn KC, Hellal F, Neukirchen D, Jacob S, Tahirovic S, Dupraz S, Stern S, Garvalov BK, Gurniak C, Shaw AE, et al. ADF/cofilin-mediated actin retrograde flow directs neurite formation in the developing brain. Neuron. 2012; 76:1091–1107. [PubMed: 23259946]

Gallardo G, Barowski J, Ravits J, Siddique T, Lingrel JB, Robertson J, Steen H, Bonni A. An alpha2-Na/K ATPase/alpha-adducin complex in astrocytes triggers non-cell autonomous neurodegeneration. Nat Neurosci. 2014; 17:1710–1719. [PubMed: 25344630]

Gallo G. More than one ring to bind them all: recent insights into the structure of the axon. Dev Neurobiol. 2013; 73:799–805. [PubMed: 23784998]

Ganguly A, Tang Y, Wang L, Ladt K, Loi J, Dargent B, Leterrier C, Roy S. A dynamic formin-dependent deep F-actin network in axons. J Cell Biol. 2015; 210:401–417. [PubMed: 26216902]

Gilligan DM, Lozovatsky L, Gwynn B, Brugnara C, Mohandas N, Peters LL. Targeted disruption of the beta adducin gene (Add2) causes red blood cell spherocytosis in mice. Proc Natl Acad Sci U S A. 1999; 96:10717–10722. [PubMed: 10485892]

Hammarlund M, Jorgensen EM, Bastiani MJ. Axons break in animals lacking beta-spectrin. J Cell Biol. 2007; 176:269–275. [PubMed: 17261846]

Kevenaar JT, Hoogenraad CC. The axonal cytoskeleton: from organization to function. Front Mol Neurosci. 2015; 8:44. [PubMed: 26321907]

Kruer MC, Jepperson T, Dutta S, Steiner RD, Cottenie E, Sanford L, Merkens M, Russman BS, Blasco PA, Fan G, et al. Mutations in gamma adducin are associated with inherited cerebral palsy. Ann Neurol. 2013; 74:805–814. [PubMed: 23836506]

Leite SC, Sousa MM. The neuronal and actin commitment: Why do neurons need rings? Cytoskeleton (Hoboken). 2016 10.1002/cm.21273.

Li X, Matsuoka Y, Bennett V. Adducin preferentially recruits spectrin to the fast growing ends of actin filaments in a complex requiring the MARCKS-related domain and a newly defined oligomerization domain. J Biol Chem. 1998; 273:19329–19338. [PubMed: 9668123]

Lukinavicius G, Reymond L, D'Este E, Masharina A, Gottfert F, Ta H, Guther A, Fournier M, Rizzo S, Waldmann H, et al. Fluorogenic probes for live-cell imaging of the cytoskeleton. Nat Methods. 2014; 11:731–733. [PubMed: 24859753]

Matsuoka Y, Li X, Bennett V. Adducin: structure, function and regulation. Cell Mol Life Sci. 2000; 57:884–895. [PubMed: 10950304]

Mische SM, Mooseker MS, Morrow JS. Erythrocyte adducin: a calmodulin-regulated actin-bundling protein that stimulates spectrin-actin binding. J Cell Biol. 1987; 105:2837–2845. [PubMed: 3693401]

Mohandas N, Gallagher PG. Red cell membrane: past, present, and future. Blood. 2008; 112:3939–3948. [PubMed: 18988878]

Pathak D, Sepp KJ, Hollenbeck PJ. Evidence that myosin activity opposes microtubule-based axonal transport of mitochondria. J Neurosci. 2010; 30:8984–8992. [PubMed: 20592219]

Pielage J, Bulat V, Zuchero JB, Fetter RD, Davis GW. Hts/Adducin controls synaptic elaboration and elimination. Neuron. 2011; 69:1114–1131. [PubMed: 21435557]

Riedl J, Crevenna AH, Kessenbrock K, Yu JH, Neukirchen D, Bista M, Bradke F, Jenne D, Holak TA, Werb Z, et al. Lifeact: a versatile marker to visualize F-actin. Nat Methods. 2008; 5:605–607. [PubMed: 18536722]

Robledo RF, Ciciotte SL, Gwynn B, Sahr KE, Gilligan DM, Mohandas N, Peters LL. Targeted deletion of alpha-adducin results in absent beta- and gamma-adducin, compensated hemolytic anemia, and lethal hydrocephalus in mice. Blood. 2008; 112:4298–4307. [PubMed: 18723693]

Robledo RF, Seburn KL, Nicholson A, Peters LL. Strain-specific hyperkyphosis and megaesophagus in Add1 null mice. Genesis. 2012; 50:882–891. [PubMed: 22926980]

Roy S. Waves, rings, and trails: The scenic landscape of axonal actin. J Cell Biol. 2016; 212:131–134. [PubMed: 26754647]

Sinnar SA, Antoku S, Saffin JM, Cooper JA, Halpain S. Capping protein is essential for cell migration in vivo and for filopodial morphology and dynamics. Mol Biol Cell. 2014; 25:2152–2160. [PubMed: 24829386]

Stepanova T, Slemmer J, Hoogenraad CC, Lansbergen G, Dortland B, De Zeeuw CI, Grosveld F, van Cappellen G, Akhmanova A, Galjart N. Visualization of microtubule growth in cultured neurons via the use of EB3-GFP (end-binding protein 3-green fluorescent protein). J Neurosci. 2003; 23:2655–2664. [PubMed: 12684451]

Xu K, Zhong G, Zhuang X. Actin, spectrin, and associated proteins form a periodic cytoskeletal structure in axons. Science. 2013; 339:452–456. [PubMed: 23239625]

Zhong G, He J, Zhou R, Lorenzo D, Babcock HP, Bennett V, Zhuang X. Developmental mechanism of the periodic membrane skeleton in axons. Elife. 2014; 3:e04581.

Highlights

- Absence of adducin leads to progressive axon enlargement and degeneration

- In the absence of adducin, the periodicity of axonal actin rings is normal

- Adducin-deficient actin rings have an increased diameter

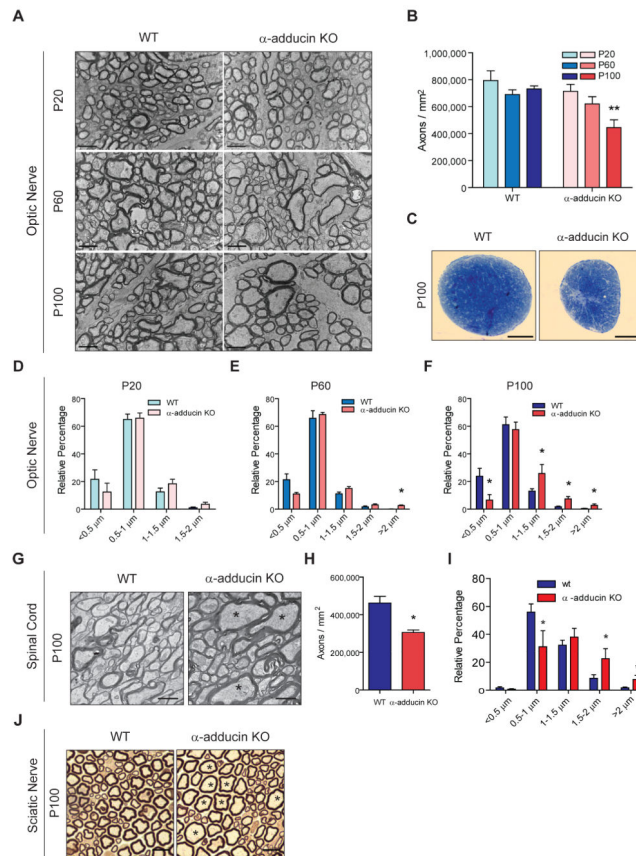- DRG neurons and retinal ganglion cells have periodic actin rings

Figure 1. α-adducin KO mice show progressive axon enlargement and axonopathy

(A) Representative 12,000x microphotographs of ultra-thin sections of optic nerves from WT and α-adducin KO mice at P20, P60 and P100; Scale bar: 2 μm.

(B) Axon density in the optic nerve of WT (P20 n=4; P60 n=5; P100 n=5) and α-adducin KO mice (P20 n=4; P60 n=5; P100 n=4). ** p<0.01.

(C) Representative semi-thin cross sections of WT and α-adducin KO optic nerves stained with toluidine blue; Scale bar: 100 μm.

(D-F) Axon distribution according to diameter in P20 (D), P60 (E) and P100 (F) WT (P20 n=5; P60 n=4; P100 n=6) and α-adducin KO (P20 n=4; P60 n=4; P100 n=5) optic nerves. p *<0.05. Graphs show mean ± s.e.m.

(G) Representative 6,000x microphotographs of ultra-thin sections of WT and α-adducin KO corticospinal tracts; asterisks (*) highlight axons with enlarged diameter; Scale bar: 1 μm.

(H) Axon density in the corticospinal tract of WT (n=4) and α-adducin KO mice (n=4) at P100. * p<0.05.

(I) Axon distribution according to diameter in P100 WT (n=4, 2237 axons measured) and α-adducin KO (n=4, 1658 axons measured) corticospinal tracts. * p<0.05.

(J) Representative semi-thin sections of WT and α-adducin KO sciatic nerves; asterisks (*) highlight axons with enlarged diameter; Scale bar: 10 μm.
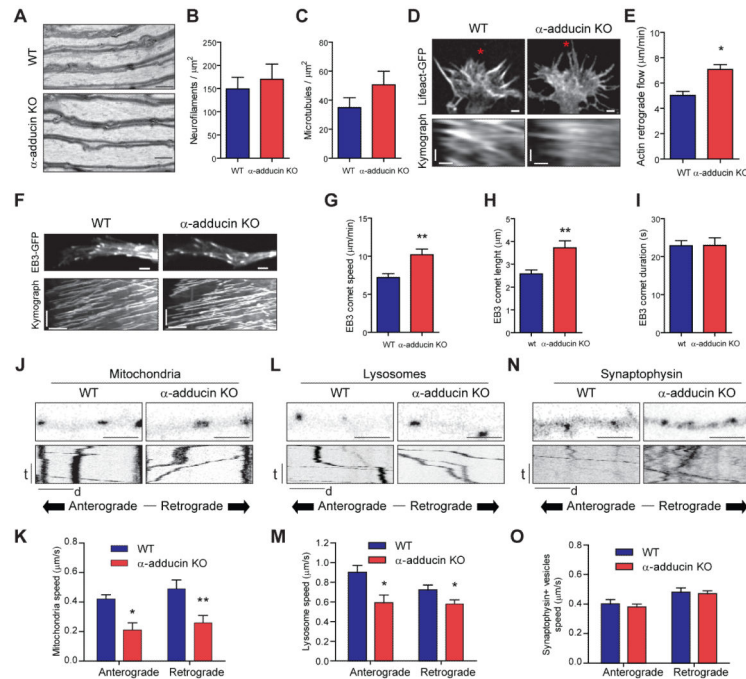
Figure 2. Loss of adducin impairs cytoskeleton dynamics in the growth cone and axonal transport

(A) Longitudinal sections of WT and α-adducin KO optic nerves (P100); Scale bar 1 μm.

(B and C) Analyses of neurofilament (B) and microtubule (C) densities in WT (n=6) and α-adducin KO (n=5) optic nerves.

(D) Representative growth cones of lifeAct-GFP transfected hippocampal neurons (upper) and respective kymographs (lower). Red asterisks highlight the region where kymographs were performed. Upper: scale bar 2 μm; Bottom: vertical scale bar- time (t): 50 seconds, horizontal scale bar- distance (d): 1 μm.

(E) Quantification of actin retrograde flow in hippocampal neurons from WT and α-adducin KO mice. * p<0.05.

(F) Representative growth cones of EB3-GFP transfected DRG neurons (upper) and respective kymographs (lower). Upper scale bar: 2 μm; Bottom: vertical scale bar- time (t): 50 seconds, horizontal scale bar- distance (d): 1 μm.

(G – I) Quantification of microtubule growth speed (G), comet length (H) and comet duration (I) in DRG neurons from WT and α-adducin KO mice. ** p<0.01.

(J-O) Analysis in WT and α-adducin KO hippocampal neurons of the axonal transport of mitochondria (J and K), lysosomes (L and M) and synaptophysin (N and O); (J, L and N) Upper – still images at t=0, Scale bar: 1μm; Lower – kymographs; vertical scale bar: time (t): 100 seconds; horizontal scale bar: distance (d): 5 μm; (K, M and O) Quantification of the speed of axonal transport. * p<0.05, ** p<0.01. Graphs show mean ± s.e.m.
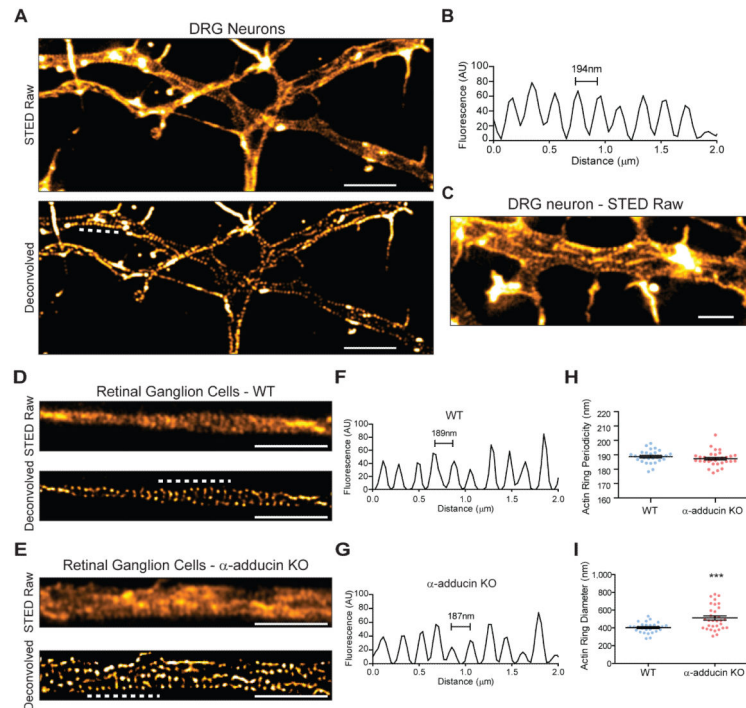
Figure 3. Lack of adducin gives rise of axon actin rings of increased diameter in RGCs

(A) STED super resolution microscopy of DIV2 rat DRG neurons stained with SiR-actin; upper- raw images, lower- deconvolved images. Scale bar: 2μm. The analysis of actin ring periodicity was performed in 16 independent axons in axonal segments of approximately 5μm.

(B) Representative fluorescence intensity profile graph of a 2 μm axonal segment of a DIV2 rat DRG neuron (obtained in the region highlighted by the dashed white line in Figure 3A, lower panel).

(C) DIV2 DRG neurons present longitudinal actin filaments, highlighted with white arrowheads. Scale bar: 1 μm.

(D and E) STED super resolution microscopy of WT (D) and α-adducin KO (E) DIV19 RGCs; upper-raw images, lower- deconvolved images. Scale bars: 2 μm.

(F-H) Analysis of the periodicity of axon actin rings in DIV19 RGCs from WT (F, H) and α-adducin KO (G, H) neurons. Measurements were performed in deconvolved images. The analysis of the periodicity of axon actin rings was performed in WT n=28; α-adducin KO n=33 independent axons in axonal segments of approximately 7μm. (F and G) Representative fluorescence intensity profile graphs of 2 μm axonal segments highlighted by the dashed white lines in Figures 3D and 3E, respectively, lower panels).

(I) Analysis of actin ring diameter in DIV19 RGCs from WT and α-adducin KO neurons. p-value ***<0.001. WT n=28; α-adducin KO n=32 axons. Graphs show mean ± s.e.m.; each dot is the average measurement for a given individual axon.
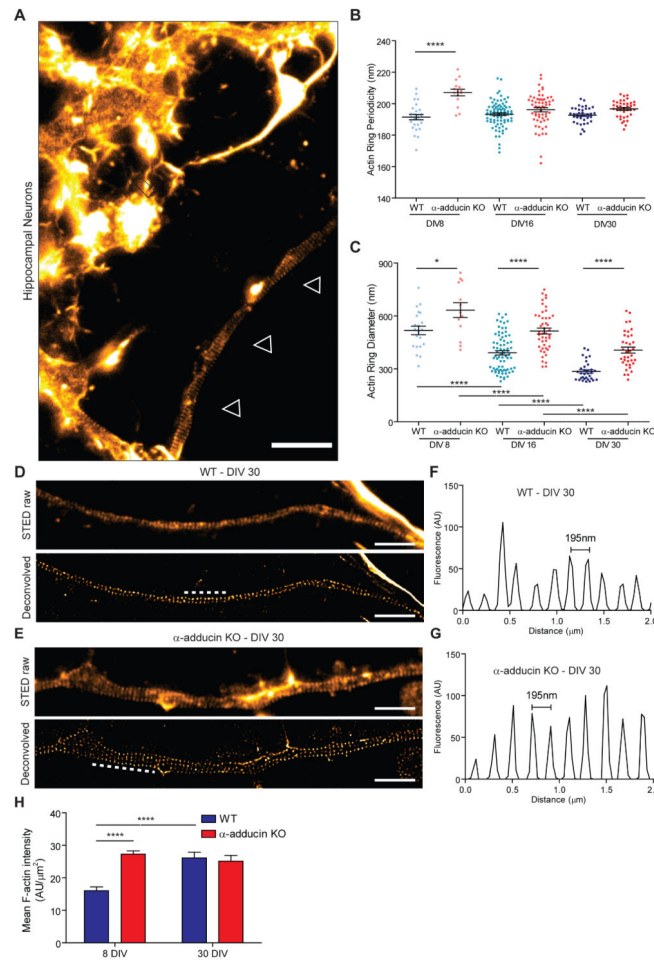
Figure 4. Analysis of axon actin rings in WT and α-adducin KO hippocampal neurons

(A) STED super resolution microscopy of DIV30 SiR-actin stained WT hippocampal neurons. One axon is highlighted with white arrowheads and dendrites are highlighted with white arrows. Scale bar: 2 μm.

(B) Analysis of actin ring periodicity in WT and α-adducin KO neurons (DIV8: WT n=26; α-adducin KO n=15; DIV16: WT n=87; α-adducin KO n=59; DIV30: WT n=37; α-adducin KO n=38 axons). The analysis of the periodicity of axon actin rings was performed in axonal segments of approximately 7μm. All measurements were done in deconvolved images. **** p<0.0001.

(C) Analysis of the actin ring diameter in DIV8, DIV16 and DIV30 in WT and α-adducin KO neurons (DIV8: WT n=21; α-adducin KO n=13; DIV16: WT n=77; α-adducin KO n=59; DIV30: WT n=37; α-adducin KO n=38 axons). * p<0.05, **** p<0.0001.

(D and E) Representative STED images of DIV30 WT (D) and α-adducin KO (E) hippocampal neurons; upper- raw images and lower- deconvolved. Scale bars: 2 μm.

(F and G) Representative fluorescence intensity profiles of 2 μm axonal segments highlighted by the dashed white lines in Figures 4D and 4E (respectively, lower panels).

(H) Analysis of the F-actin mean intensity in axonal actin rings (in arbitrary units of fluorescence per μm^2). **** $p<0.0001$. Graphs show mean ± s.e.m.; each dot is the average measurement for a given individual axon.